Spectral Fine Tuning of Cyanine Dyes: Electron Donor-Acceptor Substituted Analogues of Thiazole Orange

Journal:	*Photochemical & Photobiological Sciences*
Manuscript ID:	PP-ART-03-2015-000117.R1
Article Type:	Paper
Date Submitted by the Author:	09-Jun-2015
Complete List of Authors:	Rastede, Elizabeth; Carnegie Mellon University, Molecular Biosensor and Imaging Center; Carnegie Mellon University, Chemistry Tanha, Matteus; Carnegie Mellon University, Chemistry Yaron, David; Carnegie Mellon University, Chemistry; Carnegie Mellon University, Department of Chemistry Watkins, Simon; University of Pittsburgh, Department of Cell Biology and Center for Biologic Imaging Waggoner, Alan; Carnegie Mellon University, Molecular Biosensor and Imaging Center Armitage, Bruce; Carnegie Mellon University, Chemistry; Carnegie Mellon University, Molecular Biosensor and Imaging Center

Spectral Fine Tuning of Cyanine Dyes: Electron Donor-Acceptor Substituted Analogues of Thiazole Orange†

Elizabeth E. Rastede[a,b], Matteus Tanha[a], David Yaron[a], Simon C. Watkins,[b,c] Alan S. Waggoner[b], and Bruce A. Armitage[a,b]

[a]Department of Chemistry and [b]Molecular Biosensor and Imaging Center; Carnegie Mellon University; Pittsburgh, Pennsylvania, United States

[c]Department of Cell Biology and Center for Biologic Imaging; University of Pittsburgh; Pittsburgh, Pennsylvania, United States

Abstract: The introduction of electron donor and acceptor groups at strategic locations on a fluorogenic cyanine dye allows fine-tuning of the absorption and emission spectra while preserving the ability of the dye to bind to biomolecular hosts such as double-stranded DNA and a single-chain antibody fragment originally selected for binding to the parent unsubstituted dye, thiazole orange (TO). The observed spectral shifts are consistent with calculated HOMO-LUMO energy gaps and reflect electron density localization on the quinoline half of TO in the LUMO. A dye bearing donating methoxy and withdrawing trifluoromethyl groups on the benzothiazole and quinoline rings, respectively, shifts the absorption spectrum to sufficiently longer wavelengths to allow excitation at green wavelengths as opposed to the parent dye, which is optimally excited in the blue.

†Electronic Supporting Information Available

* Contact author: army@cmu.edu

Introduction

Fluorogenic dyes are a special class of fluorophores that show distinctly different emission intensities depending on their local environment[1-7]. For example, unsymmetrical cyanine dyes exhibit low fluorescence quantum yields in fluid solution but strongly enhanced emission in viscous solution or other environments that conformationally constrain the dyes[8, 9]. This phenomenon arises from a nonradiative twisting pathway about the central methine bridge that is inhibited when the dye is constrained[8, 10]. The unsymmetrical cyanines (Chart 1) were originally used as fluorogenic DNA stains where intercalation into the DNA base pair stack leads to >100-fold fluorescence enhancements[11-13]. Subsequently, conjugation of unsymmetrical cyanines to various classes of molecules (e.g. DNA, peptides, PNA) yielded "light-up probes" that exhibit enhanced fluorescence upon binding to another molecule[14-24]. More recently, combination of fluorogenic cyanines and other dyes with single chain antibody fragment partners has allowed creation of a modular catalogue of dye-protein complexes with absorption and emission spectra spanning most of the visible spectrum[25-34]. The dye and protein are each nonfluorescent separately, but become strongly fluorescent upon formation of a noncovalent complex, with quantum yields up to 100%[29].

Cyanine dye colors can be designed to extend over the entire visible and near-IR range through variation of the length of the central polymethine bridge (*n* = 1, 3, 5, 7, 9) and the identity of the heterocycles (e.g. dimethylindole, benzothiazole, benzoxazole, quinoline)[35, 36]. For example, each increase in bridge length (e.g. *n* = 1 to *n* = 3) results in an approximate 100 nm red shift of the absorption and emission spectra. Addition of substituents to the polymethine bridge can also result in significant spectral shifts, although conformational and electronic factors can sometimes offset one another, leading to minimal change in color[27, 30, 37, 38].

Chart 1

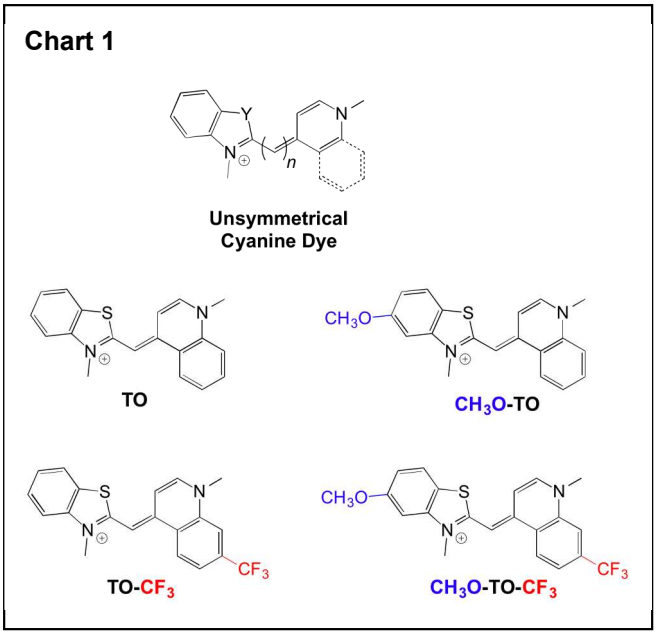

Alternatively, fine-tuning of the cyanine dye spectra can be accomplished through introduction of substituents on the aromatic heterocycles[10]. For example, substitution of electron-withdrawing fluorines for hydrogens on the benzothiazole ring of TO led to blue-shifted spectra, with the magnitude of the shift correlating with the number of fluorine atoms. On the other hand, substitution of a trifluoromethyl group on the quinoline ring of TO led to a red-shift. These observations were rationalized in terms of the frontier orbitals: the HOMO has more electron density on the benzothiazole ring, so EWGs on the benzothiazole will stabilize the HOMO more than the LUMO, leading to a larger HOMO-LUMO gap and therefore blue-shifted spectra. Conversely, EWGs on the quinoline will preferentially stabilize the LUMO, leading to a smaller HOMO-LUMO gap and red-shifted spectra.

The prior results for TO analogues lead to the prediction that EDGs on the benzothiazole ring will result in red-shifted spectra, due to preferential destabilization of the HOMO, thereby reinforcing the effects of EWGs on the quinoline ring. To test this prediction, we synthesized two new TO analogues bearing an electron-donating methoxy group on the benzothiazole ring and characterized their spectral properties computationally, in solution, and when bound to either DNA or a TO-binding protein.

Materials and Methods

General Experimental

All reagents were purchased from Sigma Aldrich or Alfa Aesar and purity was checked by H^1 NMR (300MHz). Solvents were ACS grade. 4-chloro-1-methylquinolinium iodide (Q) was obtained from Dr. N. Shank. UV-Vis spectra were recorded on a CARY-300 Bio UV-visible spectrophotometer, Fluorescence spectra were recorded on a CARY Eclipse fluorimeter, ^{1}H and ^{13}C NMR spectra were run on a Brucker Avance spectrometer at 500 and 75.47 MHz, respectively. Chemical shifts are reported as δ values (ppm) with reference to the residual solvent peaks. ESI-MS spectra were taken in a Finnigan ESI/APCI Ion Trap Mass Spectrometer on positive ion mode.

Dye Synthesis

Synthesis of 5-methoxy-2,3-dimethylbenzothiazol-3-ium iodide (CH_3O-BT). 5-methoxy-2-methylbenzothiazole (2.00 g, 11.2 mmol) was dissolved in Iodomethane (7.04 mL) and microwave irradiated for 35 minutes at 100 °C. The precipitated product was collected through

filtration and washed with cold ether and dried under vacuum. A chalky white solid was obtained (2.13 g, 60%).

^{1}H NMR (500 MHz, DMSO-d_6) δ 8.29 (d, *J* = 9.00 Hz, 1H); 7.78 (d, *J* = 2.3 Hz, 1H); 7.43 (dd, *J* = 9.0, 2.3 Hz, 1H); 4.17 (s, 3H); 3.97 (s, 3H); 3.138 (s, 3H). ^{13}C NMR (75 MHz, DMSO) δ 177.6, 161.1, 143.6, 125.6, 120.9, 118.3, 100.5, 59.9, 36.6, 17.6. *ESI-MS* (positive*) m/z* calcd for $C_{10}H_{12}NOS^+$: 194.2; Found : 194.1.

Synthesis of 1-methyl-4-(methylthio)-7-trifluoromethylquinolinium iodide ***(Q-CF$_3$).*** To a solution of 7-trifluoromethylquinolinethiol (1.00g, 4.33 mmol) dissolved in acetonitrile (5 mL), Iodomethane (326 uL, 0.037 mg, 5.19 mmol) was added under argon. After 1 hr of stirring, the product precipitated as a dark red solid. The mixture was then stirred for an additional 3 days. The resulting reaction mixture was filtered and washed with acetonitrile. The mother liquid was recrystallized using acetonitrile and the crystals were filtered and washed with cold ether. A red solid was obtained (120 mg, 15 %)

^{1}H NMR (500 MHz, DMSO-d_6) δ 9.29 (d, *J* = 6.6 Hz, 1H); 8.77(s, 1H); 8.67 (d, *J* = 8.8 Hz, 1H); 8.30 (dd, *J* = 8.8, 1.4 Hz, 1H); 8.03 (d, *J* = 6.6 Hz, 1H); 4.57 (s, 3H); 2.94 (s, 3H). ^{13}C NMR (75 MHz, DMSO) δ 164.3, 148.9, 136.6, 127.2, 125.5, 118.8, 117.7, 44.0, 15.1. *ESI-MS* (positive) *m/z* calcd for $C_{12}H_{11}F_3NS^+$: 258.1; Found: 258.2.

Synthesis of CH$_3$O-TO-CF$_3$: **CH$_3$O-BT** (33.4 mg, 0.104 mmol) and **Q-CF$_3$** (40.0 mg, 0.104 mmol) were dissolved in methanol (2 mL). Triethylamine (73.3 uL, 52.6 mg, 0.52 mmol) was added drop wise over a minute and the product precipitated as a red solid. The reaction mixture was then stirred for 17 hours. To the reaction mixture ether (15 mL) was added drop wise and a red precipitate was filtered (20 mg, 20% yield).

^{1}H NMR (500 MHz, DMSO-d_6) δ 9.03 (d, *J* = 8.9 Hz, 1H), 8.60 (d, *J* = 7.3 Hz, 1H), 8.31 (s, 1H), 8.01 (d, *J* = 8.7 Hz, 2H), 7.45 (d, *J* = 2.2 Hz, 1H), 7.34 (d, *J* = 7.2 Hz, 1H), 7.11 (dd, *J* = 8.8, 2.3 Hz, 1H), 7.03 (s, 1H), 4.21 (s, 3H), 4.11 (s, 3H), 3.95 (s, 3H). ^{13}C NMR (75 MHz, DMSO) δ 162.5, 160.8, 147.4, 146.1, 142.4, 138.5, 132.4, 127.8, 126.7, 124.1, 122.4, 116.3, 116.1, 113.6, 108.6, 99.0, 89.8, 56.6, 55.4, 42.7, 34.8. *ESI-MS* (positive*) m/z* calcd for $C_{21}H_{18}F_3N_2OS^+$: 403.1 *m/z* Found: 403.2.

Synthesis of CH$_3$O-TO: **CH$_3$O-BT** (100 mg, 0.33 mmol) and 4-chloro-1-methylquinolinium iodide, (105 mg, 0.33 mmol) were dissolved in 3mL of methanol. Triethylamine (231 uL, 1.64

mmol) was added dropwise over 2 minutes to the yellow reaction mixture. Upon the addition of TEA the reaction mixture turned dark red. The reaction was stirred for 23 hours at room temperature and 20 mL of ether was added to the reaction mixture and a red precipitate was filtered and washed with cold ether (105 mg, 67%)

^{1}H NMR (500 MHz, DMSO-d_6) δ 8.81 (d, J = 8.15 Hz, 1H); 8.59 (d, J = 7.2 Hz, 1H); 8.05 (m, 2H); 7.93 (d, J = 8.7 Hz, 1H); 7.78 (t, J = 7.8 Hz, 1H); 7.38 (d, J = 2.2 Hz, 1H); 7.33 (d, J = 7.15 Hz, 1H); 7.05 (dd, J1 = 8.7 Hz, J2 = 2.2 Hz, 1H); 6.95 (s, 1H); 4.17 (s, 3H); 4.03 (s, 3H); 3.92 (s, 3H). ^{13}C NMR (75 MHz, DMSO) δ 161.4, 160.7, 148.6, 145.4, 142.4, 138.5, 133.6, 127.3, 125.9, 124.5, 123.9, 118.7, 115.6, 112.8, 108.2, 98.8, 88.6, 56.5, 42.8, 34.4 *ESI-MS* (positive) *m/z* calcd for $C_{20}H_{19}N_2OS^+$: 335.2, Found: 335.1.

Spectroscopic Studies

Dye solutions. Dye stock solutions (~1 mM) were prepared in DMSO and stored in the dark at 0 °C; concentrations were determined using extinction coefficients reported in the literature (TO: ε_{502} = 63,000 $M^{-1}cm^{-1}$; TO-CF_3: ε_{516} = 65,000 $M^{-1}cm^{-1}$). Extinction coefficients for new compounds were determined in methanol CH_3O-TO: ε_{512} = 68,600 ± 1,100 $M^{-1}cm^{-1}$; CH_3O-TO-CF_3 : ε_{526} = 58,000 ± 2,600 $M^{-1}cm^{-1}$

DNA solutions. DNA was purchased from GE-Biosciences, calf thymus DNA (ct-DNA) was used as received. Its concentration was determined in PBS buffer at 260 nm using the manufacturer extinction coefficient (ε_{260}= 13,200 $M^{-1}cm^{-1}$) per base pair.

Protein Solutions. Soluble scFv K7 was prepared as described previously.[26] Protein concentration was determined using a Nanodrop spectrometer (ε_{280} = 36,040 $M^{-1}cm^{-1}$).

Fluorescence Quantum Yield

Fluorescence quantum yields for all dyes were determined relative to standards fluorescein and lucifer yellow, which were chosen due to their spectral overlap with TO analogs ($\Phi_{fluorescein}$ = 0.79 in 0.1 N NaOH[39]; $\Phi_{lucifer\ yellow}$ = 0.21 in nanopure H_2O at 22 °C[40]). Serial dilutions of the standards were made and the absorbance and fluorescence (ex 470) were measured. Fluorescence and absorbance measurements were performed with the dye in a solution of 90% glycerol in water as well as dye in the presence of excess soluble protein or calf thymus DNA. All standard and

sample solutions had a maximum absorbance that did not exceed 0.1. All measurements were performed in triplicate to determine mean quantum yields and standard deviations.

Each fluorescence spectrum was integrated using Origin software. Then the integrated fluorescence intensity was plotted vs absorbance at 470 nm and a trendline calculated with y intercept = 0. The slope of this line is the gradient (*grad*). Using the gradient of the unknown (*grad x*) as well as the standard ($grad_{std}$) in addition to the refractive index of their respective solvents (*n*), the unknown quantum yield (Φ_x) was determined using the equation below.

$$\Phi_x = \Phi_{std} * \left(\frac{grad_x}{grad_{std}}\right) * \left(\frac{n_x}{n_{std}}\right)^2$$

Protein Binding

Range Finding Assay.[41] A serial dilution of 10:1 (dye:scFv) as well as a control serial dilution of just dye were made, starting at 10 μM dye to 2 nM. The resulting samples were allowed to equilibrate in eppendorf tubes at room temperature overnight. Then the background signal was corrected by subtracting the fluorescence intensity of just dye from the fluorescence intensity of the complex. The corrected fluorescence was multiplied by the dilution factor and then normalized. The expected results should show a definite plateau at 1, this indicates that the system is above the K_D and the assumption that a 1:1 binding relationship is true. However the point in which the normalized fluorescence decreases indicates that the system is nearing the K_D and the complex starts to dissociate. We use this curve to estimate the concentration in which half of the dye or protein is bound.

K_D Determination for Dye and Soluble FAP. For each dye, a parallel dilution series was performed using 16 different concentrations of dye that was centered around the estimated K_D (determined by range finding assay). From that dilution series two different samples were generated: a control dye in wash buffer, as well as dye:K7 in wash buffer. The concentration of K7 was kept constant for each dye sample and the experiment was performed in triplicate. The resulting data were fit using the ligand depletion model saturation binding equation in Graph Pad.

Cell Imaging

HeLa cells were plated on MatTec dishes were incubated with a 1:1000 dilution of either TO or CH_3O-TO-CF_3 for 30 minutes at 37°C in a humid tissue culture incubator at 37°C in the

presence of 9% CO_2. The dyes were washed off using 1 mL of complete DMEM. Following incubation with the dyes, the cells were imaged live using a Nikon A1 confocal microscope. Dyes were excited with a 488 nm and 561 nm laser and the emissions were collected with a band pass filter between the wavelengths of 505-550 nm and 603-678 nm, respectively. Imaging parameters were kept identical for each dish of cells. Images were processed using ImageJ software where a false color which represented the emission window was applied.

Computations

The molecular geometries of the ground electronic state were optimized using DFT with the B3LYP functional[42] and 6-31G** basis set. Vertical excitations were obtained from single-point TDDFT calculations with CAM-B3LYP/6-31G**[43], since this functional has been shown to perform well on cyanine dyes[44-46]. In addition, the correlation between the predicted and observed λ_{max} is significantly better for CAM-B3LYP than with the M06HF or PBE0 functionals or ZINDO[47] (see Supplemental Information). All calculations were performed using GAUSSIAN09[48] and included the effects of the methanol solvent through the Polarization Continuum Model (PCM)[49] .

Results and Discussion

Two new methoxy-substituted TO derivatives, CH_3O-TO and CH_3O-TO-CF_3 (Chart 1) were synthesized as their iodide salts by a standard route[50]: (A) *N*-methylation of 5-methoxy-2-methylbenzothiazole, (B) methylation of either 7-(trifluoromethyl)quinoline-4-thiol or 4-chloroquinoline, and (C) condensation in the presence of triethylamine to yield the final dyes (Scheme 1).

Scheme 1

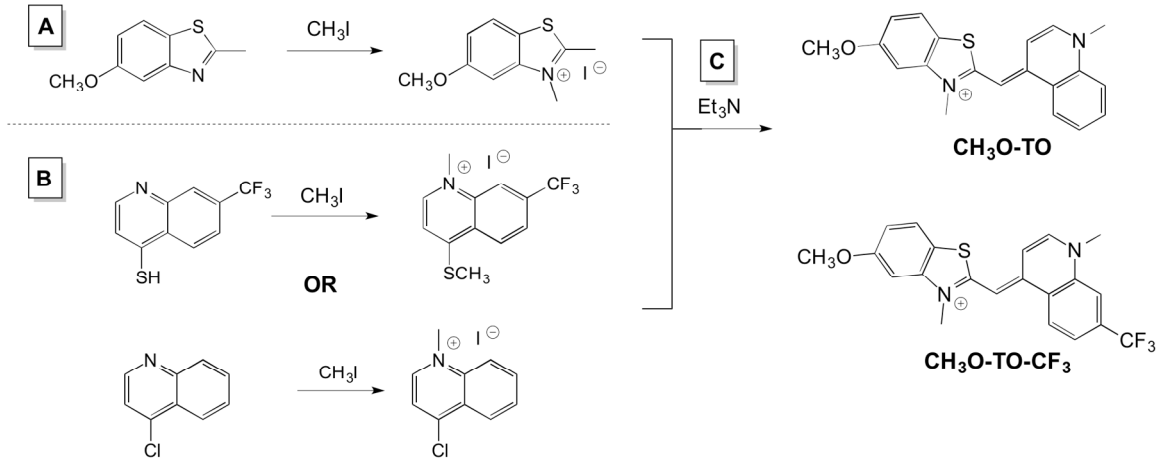

Figure 1 shows the calculated frontier orbitals for TO, along with the effects of the substituents on the HOMO and LUMO energies and on the excitations energies predicted by TDDFT. The trends in the HOMO-LUMO gaps correlate well with the excitation energies, such that the spectral shifts can be understood in terms of the effects of the substituents on the frontier orbitals. These effects are consistent with EWGs (F and CF_3) preferentially stabilizing, and EDGs (methoxy) preferentially destabilizing, the frontier orbital whose density is largest on the heterocycle to which the group is attached. Fluorine substitution on the benzothiazole thus preferentially stabilizes the HOMO and leads to blue-shifted absorption, while CF_3 substitution on the quinoline preferentially stabilizes the LUMO and leads to red-shifted absorption. Methoxy substitution on the benzothiazole preferentially destabilizes the HOMO, leading to red-shifted absorption, as observed previously by Ivanov and co-workers.[51] The substituent effects reinforce one another in CH_3O-TO-CF_3, leading to the largest red shift (Table 1).

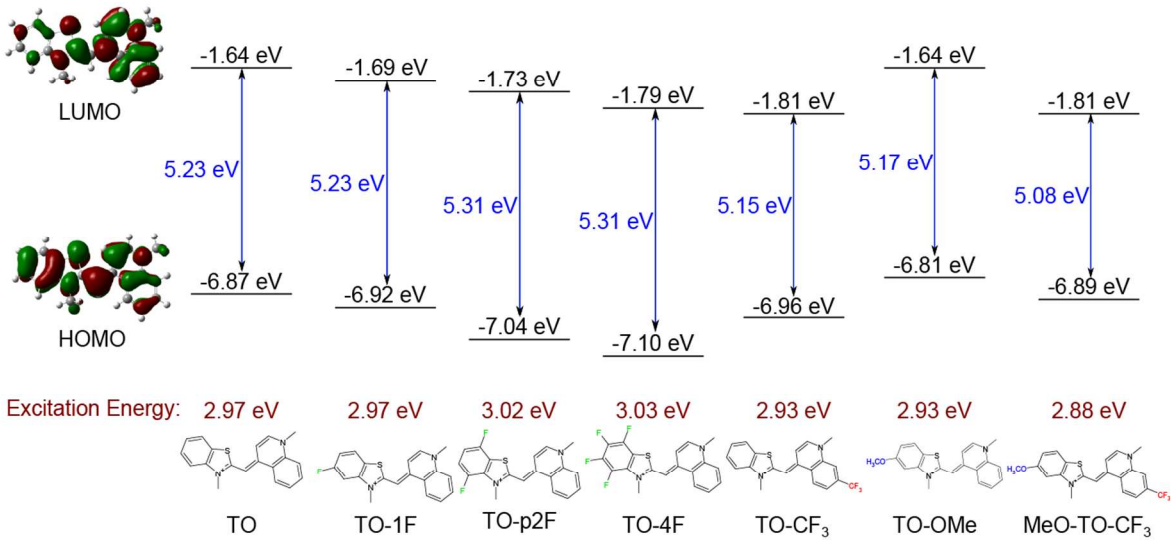

Figure 1. Frontier orbital analysis for TO and its donor/acceptor substituted analogues, including HOMO and LUMO orbitals of TO (far left), HOMO and LUMO energies (black), HOMO-LUMO gaps (blue arrows) and TDDFT excitation energies (red text).

Normalized UV-vis spectra for the new TO derivatives in methanol solution are shown in Figure 2A, along with the spectra for TO and the previously reported TO-CF_3. Trifluoromethylation of the quinoline group causes a 14 nm red shift in the absorption spectrum relative to TO. Introduction of a methoxy group at position 5 on the benzothiazole heterocycle causes a similar red shift of 10 nm, and the combination of both substituents, methoxy on the benzothiazole and trifluoromethyl on the quinoline, shows an additive effect with a red shift of 24 nm (Table 1). In Figure 2B we see that there is a good correlation between predicted and experimentally observed absorption λ_{max} values.

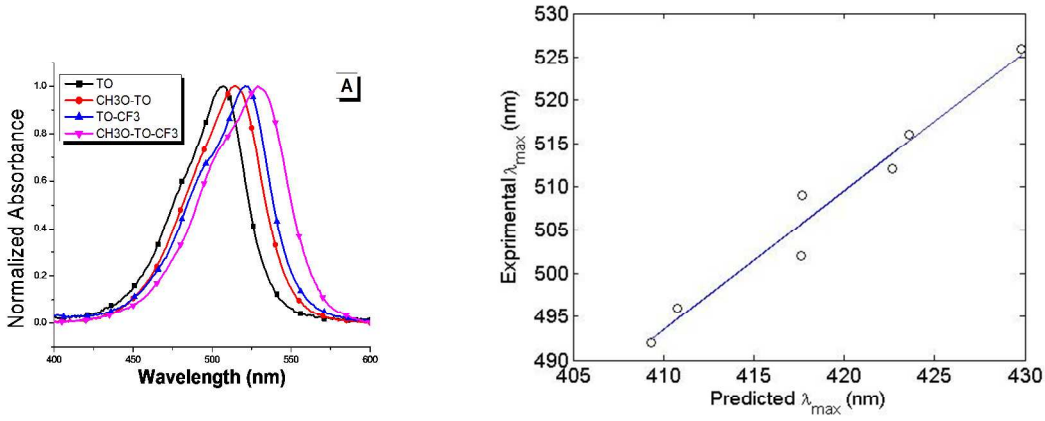

Figure 2. (A) Normalized absorbance spectra of TO dyes (1uM) in methanol. (B) Plot of experimental and predicted λ_{max} values for TO dyes. Data are included for fluorinated TO dyes reported previously.

Similar results were observed in fluorescence emission spectra recorded for the dyes (Figure 3 and Table 1). Since TO and its analogues exhibit very low fluorescence in fluid solution, we measured emission spectra in a viscous solvent consisting of 90% glycerol in water. The spectra are relatively broad, but the emission clearly red-shifts in the order TO < TO-CF_3 ≈ CH_3O-TO < CH_3O-TO-CF_3.

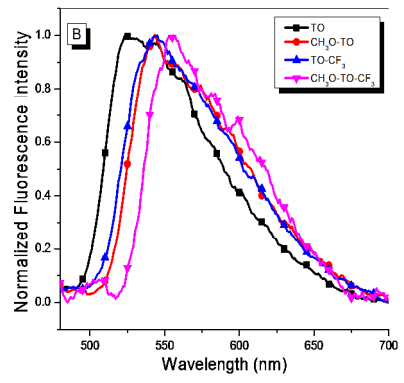

Figure 3. Normalized fluorescence spectra of TO dyes (1uM) in 90% glycerol in water.

Table 1. Extinction coefficients, wavelength maxima (nm) and fluorescence quantum yields for TO dyes in homogeneous solution.

Dye	ε ($M^{-1}cm^{-1}$)[a]	λ_{max}[a]	Em λ_{max}[b]	ϕ_f[b]
TO	68,000	502	529	0.013
CH_3O-TO	68,600	512	545	0.009
TO-CF_3	65,000	516	547	0.009
CH_3O-TO-CF_3	58,000	526	560	0.007

[a] in methanol, [b] in 90% glycerol in water

The fluorescence quantum yields were also determined for TO analogs in 90% glycerol in water (Table 1; the values for TO and TO-CF_3 are lower than we previously reported; this could be due to slight variation in the glycerol content.) As previously reported the addition of the trifluoromethyl group to the quinoline side decreases the quantum yield due to reduction in the activation barrier for twisting about the central methine in the excited state. Addition of a methoxy substituent to the benzothiazole group also decreases the quantum yield, and when both substituents are present the quantum yield decreases further.

The noncovalent binding interactions between the TO analogues and two biomolecular hosts, namely double-stranded DNA and a single-chain antibody fragment (scFv) protein called K7, which was previously shown to bind to a range of unsymmetrical cyanine dyes, were also investigated. K_D values for the four dyes to K7 are all in the low nanomolar range (Table 2). Figure 4 shows unnormalized absorbance spectra for the four dyes in glycerol/water or excess DNA or K7. The spectra exhibit the same progressive red-shift as the donor-acceptor nature of the substituents increases that was evident in methanol. Also, all four dyes exhibit greater vibronic structure upon binding to DNA and K7, as evidenced by the more prominent short wavelength shoulders observed in the corresponding absorbance spectra compared with the glycerol spectra, indicating that the dyes experience a narrower range of conformations when bound to the biopolymers.

Table 2. Wavelength maxima (nm), fluorescence quantum yields and binding affinities for TO dyes in the presence of DNA and a dye-binding protein.

Dye	λ_{A}□□□□□□□□□□	ϕ_f (DNA)	λ_{A}□□□□□□□□Protein□	ϕ_f (Protein)	K_D (Protein)[a]
TO	511/528	0.14	502/518	0.17	2.1 ± 0.5
CH_3O-TO	520/543	0.10	511/534	0.11	3.8 ± 0.6
TO-CF_3	527/548	0.05	516/535	0.21	1.0 ± 0.2
CH_3O-TO-CF_3	536/561	0.04	527/548	0.17	5.4 ± 1.2

[a] K_D values in nM

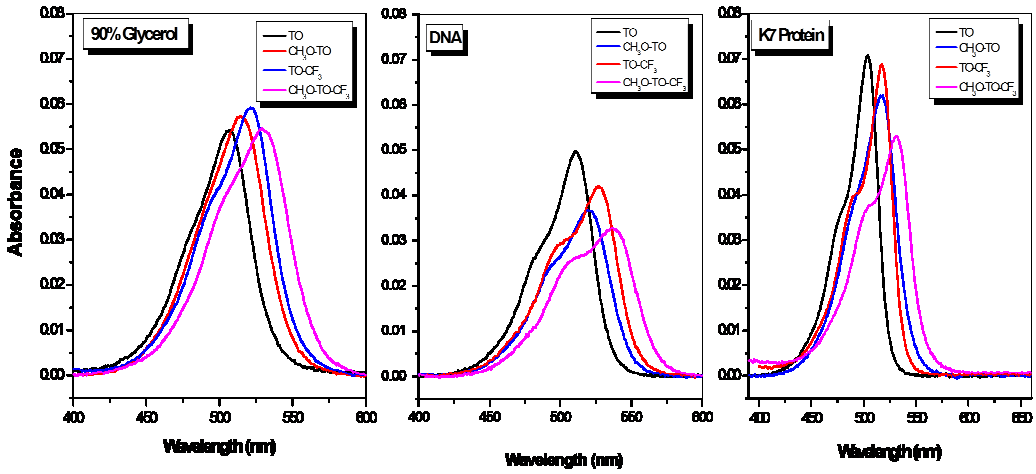

Figure 4. Visible absorbance spectra for TO dyes recorded in 90% glycerol (left), calf thymus DNA (middle) or K7 scFv protein (right). [Dye] = 1 μM, [DNA] = 100 μM base pairs, [K7] = 1 μM.

Fluorescence spectra recorded for the four dyes in methanol, glycerol, DNA and K7 protein are overlaid in Figure 5. The spectra were corrected for absorbance differences at the excitation wavelength and therefore reflect differences in quantum yields. In all four cases, the brightest fluorescence is observed when the dye is bound to the scFv protein, with intensities 10-20-fold brighter than in glycerol. Relative to TO, substitution with CH_3O causes approximately 2-fold decrease in fluorescence for both DNA and K7. In contrast, substitution with CF_3 results in nearly 2-fold *increase* in K7 fluorescence but 5-fold *decrease* in DNA fluorescence relative to TO. The disubstituted dye exhibits K7 fluorescence that is comparable to TO, but the lowest

DNA fluorescence of any of the dyes. Overall, these results indicate that the protein tolerates both substituents reasonably well, but methoxy substitution on the benzothiazole ring is detrimental to fluorescence activation by DNA. (Under the conditions of the experiment, all dyes were completely bound by the DNA and protein, so the differences in intensities reflect quantum yield differences rather than affinity differences.)

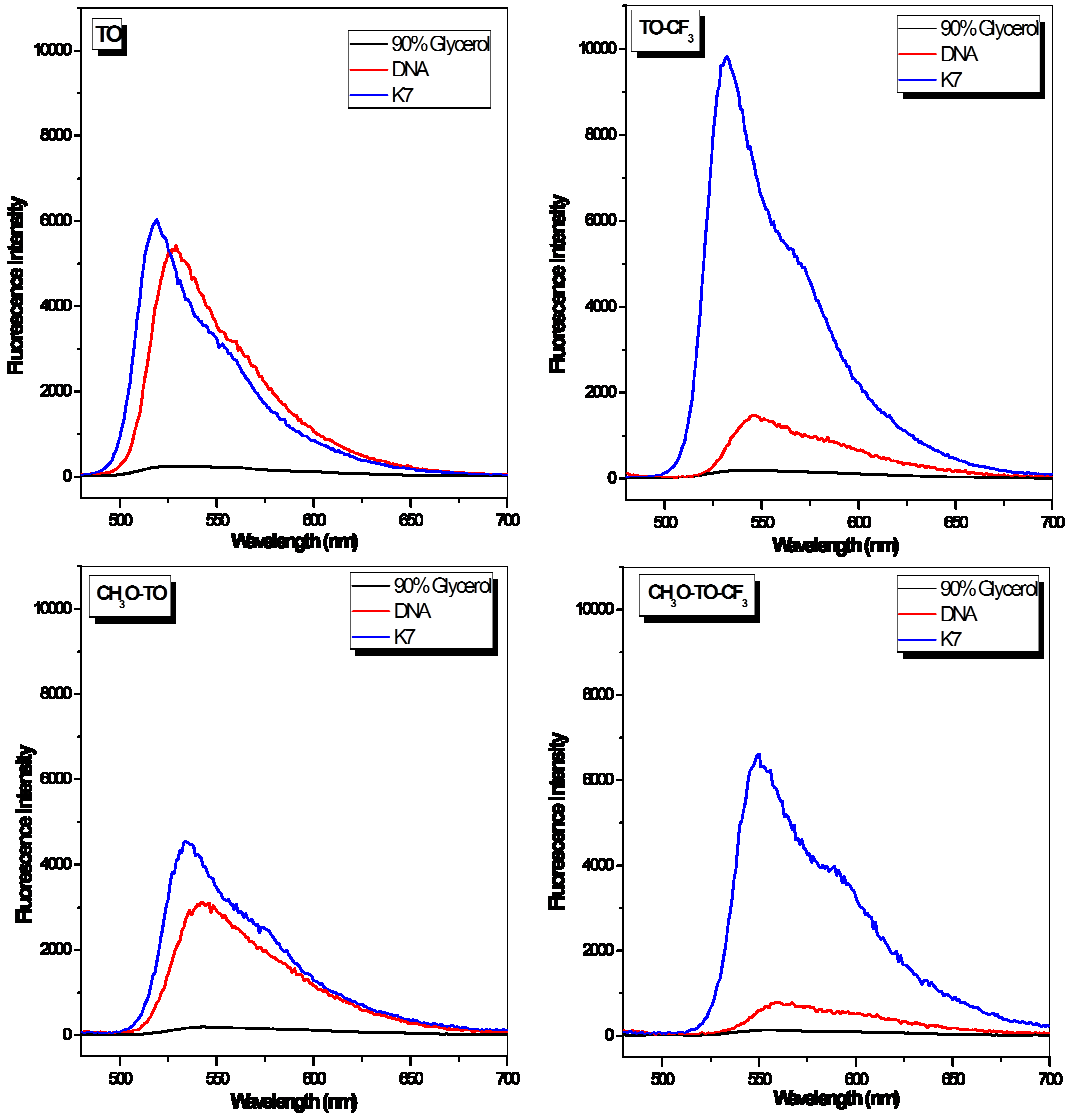

Figure 5. Fluorescence spectra for the four dyes recorded in 90% glycerol (blue), calf thymus DNA (red) or K7 scFv protein (violet). [Dye] = 1 μM, [DNA] = 100 μM base pairs, [K7] = 1 μM. λ_{ex} = 470 nm; spectra were corrected for differences in absorbance.

The red-shifted fluorescence exhibited by CH_3O-TO-CF_3 is of practical significance. In particular, whereas TO is efficiently excited by a 488 nm laser, CH_3O-TO-CF_3 can be excited by a 561 nm laser with greater than 60-fold higher extinction coefficient than TO (Table 3), more than compensating for the lower quantum yields for CH_3O-TO-CF_3 (Table 2). Thus, fine-tuning of the TO absorption spectrum through the rational introduction of donor and acceptor groups allows different excitation sources to be used without significantly changing the dye structure, permitting promiscuous receptors such as the K7 protein to be used as a multi-color fluorescent tag differentiated by the fluorogenic dye used for imaging.

In order to visually demonstrate the spectral fine tuning potential of these dyes, we tested the two extrema, TO and CH_3O-TO-CF_3, as stains for mammalian cells. We imaged HeLa cells stained with 500 nM dye without washing at two different excitation wavelengths, 488 and 561 nm. As seen in Figure 6, the dyes stain both nuclei and cytoplasm, similar to other fluorogenic cyanines.[52, 53] As expected, TO gives brighter staining upon excitation at 488 nm while CH_3O-TO-CF_3 is significantly brighter for 561 nm excitation.

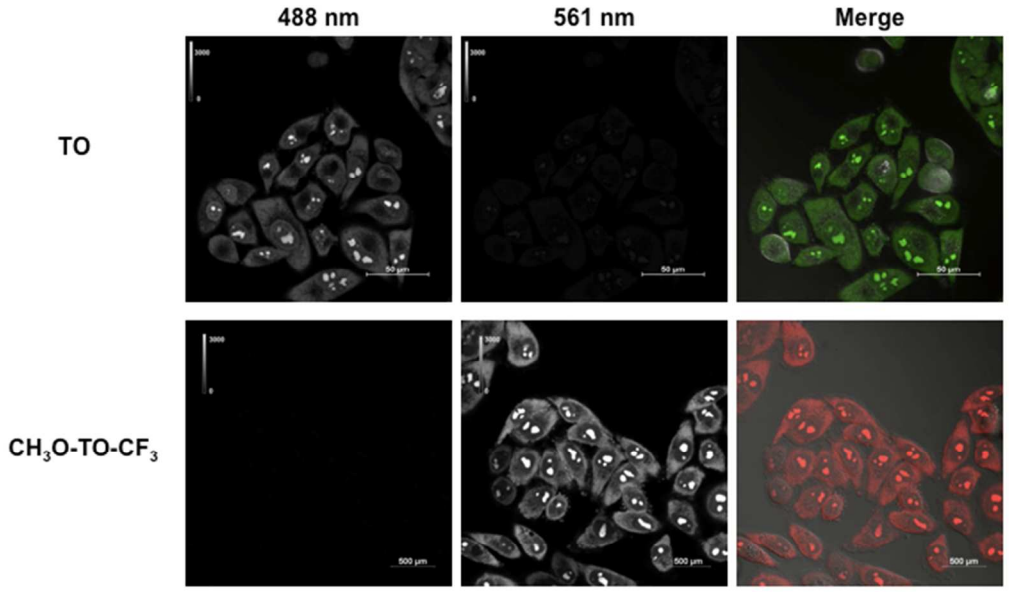

Figure 6. Fluorescence images of **TO** and **CH_3O-TO-CF_3** with HeLa cells excited at 488 nm (left panel) and 561 nm (middle panel). The overlay image combines the DIC with fluorescence from excitation at both 488 nm (false colored green) and 561 nm (false colored red). Samples were not washed before imaging. [Dye] = 500 nM.

Table 3. Extinction coefficients (M^{-1} cm^{-1}) at common laser wavelengths of TO dyes bound to CT DNA and scFv protein K7

	CT DNA			scFv protein K7		
Dye	ε_{488}	ε_{532}	ε_{561}	ε_{488}	ε_{532}	ε_{561}
TO	30,000	11,000	160	44,000	3,800	120
CH_3O-TO	22,000	27,000	1,100	40,000	30,000	1,700
TO-CF_3	22,000	40,000	2,700	43,000	26,000	476
CH_3O-TO-CF_3	15,000	32,000	10,000	25,000	48,000	6,800

Conclusion

The results reported here show the synthesis and spectral characterization of a family of fluorogenic cyanine dyes with strategic placement of electron donating and withdrawing groups in order to finely tune the absorbance and fluorescence spectra. Whereas methoxy groups were used in the present case, additional tuning of the spectra could be achieved using other donor (e.g. amino) and/or acceptor (e.g. cyano) groups placed at appropriate positions on the heterocyclic ring systems. The new TO derivatives retained, to varying degrees, the fluorogenicity and DNA/protein binding properties of the parent dye. The ability to precisely adjust the excitation and emission wavelengths without eliminating specific biomolecule binding properties can be used to optimize fluorescent labeling reagents for microscopy and cytometry applications.

Acknowledgment

This work was supported by the U.S. National Institutes of Health (grant U54 RR022241). NMR instrumentation at Carnegie Mellon University was partially supported by the NSF (CHE-0130903). Mass spectrometers were funded by NSF (DBI-9729351). Computational work was funded by NSF (CHE-1027985). We are grateful to Morgan Jessup of the Center for Biologic Imaging at the University of Pittsburgh for technical assistance with cell imaging.

References

1. L. D. Lavis and R. T. Raines, Bright Ideas for Chemical Biology, *ACS Chem. Biol.*, 2008, **3**, 142-155.

2. A. Nadler and C. Schultz, The power of fluorogenic probes, *Angew. Chem., Int. Ed.* , 2013, **52**, 2408-2410.

3. M. G. Pawar and S. G. Srivatsan, An Environment-Responsive Fluorescent Nucleoside Analog Probe for Studying Oligonucleotide Dynamics in a Model Cell-Like Compartment, *J. Phys. Chem. B*, 2013, **117**, 14273-14282.

4. E. H. Suh, Y. Liu, S. Connelly, J. C. Genereux, I. A. Wilson and J. W. Kelly, Stilbene Vinyl Sulfonamides as Fluorogenic Sensors of and Traceless Covalent Kinetic Stabilizers of Transthyretin that Prevent Amyloidogenesis, *J. Am. Chem. Soc.*, 2013, **135**, 17869-17880.

5. J. S. Paige, K. Y. Wu and S. R. Jaffrey, RNA Mimics of Green Fluorescent Protein, *Science*, 2011, **333**, 642-646.

6. E. W. Debler, G. F. Kaufmann, M. M. Meijler, A. Heine, J. M. Mee, G. Pljevaljcic, A. J. Di Bilio, P. G. Schultz, M. D. P., K. D. Janda, I. A. Wilson, H. B. Gray and R. A. Lerner, Deeply Inverted Electron-Hole Recombination in a Luminescent Antibody-Stilbene Complex, *Science*, 2008, **319**, 1232-1235.

7. X. Li, X. Gao, W. Shi and H. Ma, Design strategies for water-soluble small molecular chromogenic and fluorogenic probes, *Chem. Rev.*, 2014, **114**, 590-659.

8. J. Cao, T. Wu, C. Hu, T. Liu, W. Sun, J. Fan and X. Peng, The nature of the different environmental sensitivity of symmetrical and unsymmetrical cyanine dyes: an experimental and theoretical study, *Phys. Chem. Chem. Phys.*, 2012, **14**, 13702-13708.

9. A. Biancardi, T. Biver, A. Marini, B. Mennucci and F. Secco, Thiazole orange (TO) as a light-switch probe: a combined quantum-mechanical and spectroscopic study, *Phys. Chem. Chem. Phys.*, 2011, **13**, 12595-12602.

10. G. L. Silva, V. Ediz, D. Yaron and B. A. Armitage, Experimental and Computational Investigation of Unsymmetrical Cyanine Dyes: Understanding Torsionally Responsive Fluorogenic Dyes, *J. Am. Chem. Soc.*, 2007, **129**, 5710-5718.

11. L. G. Lee, C. Chen and L. Chiu, Thiazole Orange: A New Dye for Reticulocyte Analysis *Cytometry*, 1986, **7**, 508-517.

12. S. C. Benson, R. A. Mathies and A. N. Glazer, Heterodimeric DNA-binding dyes designed for energy transfer: stability and applications of the DNA complexes, *Nucleic Acids Res.*, 1993, **21**, 5720-5726.

13. R. M. Martin, H. Leonhardt and M. C. Cardoso, DNA labeling in living cells, *Cytometry. Part A : the journal of the International Society for Analytical Cytology*, 2005, **67**, 45-52.

14. J. Nygren, N. Svanvik and M. Kubista, The Interactions Between the Fluorescent Dye Thiazole Orange and DNA, *Biopolymers*, 1998, **46**, 39–51.

15. N. Svanvik, G. Westman, D. Wang and M. Kubista, Light-up probes: thiazole orange-conjugated peptide nucleic acid for detection of target nucleic acid in homogeneous solution, *Anal. Biochem.*, 2000, **281**, 26-35.

16. N. Svanvik, J. Nygren, G. Westman and M. Kubista, Free-Probe Fluorescence of Light-up Probes, *J. Am. Chem. Soc.*, 2001, **123**, 803-809.

17. J. R. Carreon, K. P. Mahon, Jr. and S. O. Kelley, Thiazole orange-peptide conjugates: sensitivity of DNA binding to chemical structure, *Org. Lett.*, 2004, **6**, 517-519.

18. O. Kohler, D. V. Jarikote and O. Seitz, Forced intercalation probes (FIT Probes): thiazole orange as a fluorescent base in peptide nucleic acids for homogeneous single-nucleotide-polymorphism detection, *ChemBioChem*, 2005, **6**, 69-77.

19. B. A. Armitage, Cyanine Dye–DNA Interactions: Intercalation, Groove Binding,and Aggregation, *Top. Curr. Chem.*, 2005, **253**, 55-76.

20. T. P. Constantin, G. L. Silva, K. L. Robertson, T. P. Hamilton, K. Fague, A. S. Waggoner and B. A. Armitage, Synthesis of New Fluorogenic Cyanine Dyes and Incorporation into RNA Fluoromodules, *Org. Lett.*, 2008, **10**, 1561-1564.

21. B. Ditmangklo, C. Boonlua, C. Suparpprom and T. Vilaivan, Reductive alkylation and sequential reductive alkylation-click chemistry for on-solid-support modification of pyrrolidinyl peptide nucleic acid, *Bioconjugate Chem.*, 2013, **24**, 614-625.

22. F. Hovelmann, I. Gaspar, A. Ephrussi and O. Seitz, Brightness enhanced DNA FIT-probes for wash-free RNA imaging in tissue, *J. Am. Chem. Soc.*, 2013, **135**, 19025-19032.

23. B. Xu, X. Wu, E. K. Yeow and F. Shao, A single thiazole orange molecule forms an exciplex in a DNA i-motif, *Chem. Commun.*, 2014, **50**, 6402-6405.

24. F. Hovelmann, I. Gaspar, S. Loibl, E. A. Ermilov, B. Roder, J. Wengel, A. Ephrussi and O. Seitz, Brightness through local constraint--LNA-enhanced FIT hybridization probes for in vivo ribonucleotide particle tracking, *Angew. Chem., Int. Ed.* , 2014, **53**, 11370-11375.

25. C. Szent-Gyorgyi, B. F. Schmidt, Y. Creeger, G. W. Fisher, K. L. Zakel, S. Adler, J. A. Fitzpatrick, C. A. Woolford, Q. Yan, K. V. Vasilev, P. B. Berget, M. P. Bruchez, J. W. Jarvik and A. Waggoner, Fluorogen-activating single-chain antibodies for imaging cell surface proteins, *Nat. Biotechnol.*, 2008, **26**, 235-240.

26. H. Özhalici-Ünal, C. Lee Pow, S. A. Marks, L. D. Jesper, G. L. Silva, N. I. Shank, E. W. Jones, J. M. Burnette, III, P. B. Berget and B. A. Armitage, A Rainbow of Fluoromodules: A Promiscuous scFv Protein Binds to and Activates a Diverse Set of Fluorogenic Cyanine Dyes, *J. Am. Chem. Soc.*, 2008, **130**, 12620-12621.

27. N. I. Shank, K. J. Zanotti, F. Lanni, P. B. Berget and B. A. Armitage, Enhanced Photostability of Genetically Encodable Fluoromodules Based on Fluorogenic Cyanine Dyes and a Promiscuous Protein Partner, *J. Am. Chem. Soc.*, 2009, **131**, 12961-12969.

28. C. Szent-Gyorgyi, B. F. Schmidt, A. J. Fitzpatrick and M. P. Bruchez, Fluorogenic Dendrons with Multiple Donor Chromophores as Bright Genetically Targeted and Activated Probes, *J. Am. Chem. Soc.*, 2010, **132**, 11103–11109.

29. K. J. Zanotti, G. L. Silva, Y. Creeger, K. L. Robertson, A. S. Waggoner, P. B. Berget and B. A. Armitage, Blue fluorescent dye-protein complexes based on fluorogenic cyanine dyes and single chain antibody fragments, *Org. Biomol. Chem.*, 2011, **9**, 1012-1020.

30. N. I. Shank, H. H. Pham, A. S. Waggoner and B. A. Armitage, Twisted cyanines: a non-planar fluorogenic dye with superior photostability and its use in a protein-based fluoromodule, *J. Am. Chem. Soc.*, 2013, **135**, 242-251.

31. Q. Yan, B. F. Schmidt, L. A. Perkins, M. Naganbabu, S. Saurabh, S. K. Andrekob and M. P. Bruchez, Near-instant surface-selective fluorogenic protein quantification using sulfonated triarylmethane dyes and fluorogen activating proteins, *Org. Biomol. Chem.*, 2015, DOI: 10.1039/C1034OB02309A.

32. Y. Wang, C. A. Telmer, B. F. Schmidt, J. D. Franke, S. Ort, D. J. Arndt-Jovin and M. P. Bruchez, Fluorogen Activating Protein−Affibody Probes: Modular, No-Wash Measurement of Epidermal Growth Factor Receptors, *Bioconjugate Chem.*, 2014, DOI: 10.1021/bc500525b.

33. S. L. Schwartz, Q. Yan, C. A. Telmer, K. A. Lidke, M. P. Bruchez and D. S. Lidke, Fluorogen-Activating Proteins Provide Tunable Labeling Densities for Tracking FcepsilonRI Independent of IgE, *ACS Chem. Biol.*, 2014, DOI: 10.1021/cb5005146.

34. M. J. Saunders, E. Block, A. Sorkin, A. S. Waggoner and M. P. Bruchez, A bifunctional converter: fluorescein quenching scFv/fluorogen activating protein for photostability and improved signal to noise in fluorescence experiments, *Bioconjugate Chem.*, 2014, **25**, 1556-1564.

35. A. Mishra, R. K. Behera, P. K. Behera, B. K. Mishra and G. B. Behera, Cyanines during the 1990s: A Review, *Chem. Rev.*, 2000, **100**, 1973−2011.

36. R. P. Haugland, The Molecular Probes Handbook—A Guide to Fluorescent Probes and Labeling Technologies, Molecular Probes, Eugene, OR, 2010.---

37. J. Cao, C. Hu, W. Sun, Q. Xu, J. Fan, F. Song, S. Sun and X. Peng, The mechanism of different sensitivity of meso-substituted and unsubstituted cyanine dyes in rotation-restricted environments for biomedical imaging applications, *RSC Adv.*, 2014, **4**, 13385–13394.

38. A. Toutchkine, D. V. Nguyen and K. M. Hahn, Merocyanine Dyes with Improved Photostability, *Org. Lett.*, 2007, **9**, 2775-2777.

39. A. M. Brouwer, Standards for photoluminescence quantum yield measurements in solution (IUPAC Technical Report), *Pure App. Chem.* , 2011, **83**, 2213–2228.

40. W. W. Stewart, Synthesis of 3,6-Disulfonated 4-Aminonaphthalimides, *J. Am. Chem. Soc.*, 1981, **103**, 7615-7620.

41. N. Senutovitch, R. L. Stanfield, S. Bhattacharyya, G. S. Rule, I. A. Wilson, B. A. Armitage, A. S. Waggoner and P. B. Berget, A Variable Light Domain Fluorogen Activating Protein Homodimerizes to Activate Dimethylindole Red, *Biochemistry*, 2012, **51**, 2471-2485.

42. A. D. Becke, Density-functional thermochemistry. III. The role of exact exchange, *J. Chem. Phys.*, 1993, **98**, 5648.

43. T. Yanai, D. P. Tew and N. C. Handy, A new hybrid exchange–correlation functional using the Coulomb-attenuating method (CAM-B3LYP), *Chem. Phys. Lett.*, 2004, **393**, 51-57.

44. D. Jacquemin, Y. Zhao, R. Valero, C. Adamo, I. Ciofini and D. G. Truhlar, Verdict: Time-Dependent Density Functional Theory "Not Guilty" of Large Errors for Cyanines, *J. Chem. Theory Comput.*, 2012, **8**, 1255-1259.

45. D. Jacquemin, E. A. Perpète, I. Ciofini and C. Adamo, Assessment of the ωB97 family for excited-state calculations, *Theor. Chem. Acc.*, 2010, **128**, 127-136.

46. D. Jacquemin, E. A. Perpète, G. E. Scuseria, I. Ciofini and C. Adamo, TD-DFT Performance for the Visible Absorption Spectra of Organic Dyes: Conventional versus Long-Range Hybrids, *J. Chem. Theory Comput.*, 2008, **4**, 123-135.

47. A. Tomlinson and D. Yaron, Direct INDO/SCI method for excited state calculations., *J. Comput. Chem.* , 2003, **24**, 1782-1788.

48. *Gaussian 09, Revision A.1, Frisch, M. J. et al, Wallingford CT*, 2009.

49. J. Tomasi, B. Mennucci and E. Cancès, The IEF version of the PCM solvation method: an overview of a new method addressed to study molecular solutes at the QM ab initio level, *J. Mol. Struct.*, 1999, **464**, 211-226.

50. A. J. Winstead, N. Fleming, K. Hart and D. Toney, Microwave Synthesis of Quaternary Ammonium Salts, *Molecules*, 2008, **13**, 2107-2113.

51. I. I. Timcheva, V. A. Maximova, T. G. Deligeorgiev, N. I. Gadjev, R. W. Sabnis and I. G. Ivanov, Fluorescence Spectral Characteristics of Novel Asymmetric Monomethine Cyanine Dyes in Nucleic Acid Solutions, *FEBS Lett.*, 1997, **405**, 141-144.

52. S. Zhang, J. Fan, Z. Li, N. Hao, J. Cao, T. Wu, J. Wang and X. Peng, A Bright Red Fluorescent Cyanine Dye for Live-Cell Nucleic Acid Imaging, with High Photostability and a Large Stokes Shift, *J. Mat. Chem. B*, 2014, **2**, 2688-2693.

53. R. Horobin, Where Do Dyes Go Inside Living Cells? Predicting Uptake, Intracellular Localisation, and Accumulation Using QSAR Models, *Color.Technol.*, **130**, 155-173.